Engineering Notes

ENGINEERING NOTES are short manuscripts describing new developments or important results of a preliminary nature. These Notes cannot exceed 6 manuscript pages and 3 figures; a page of text may be substituted for a figure and vice versa. After informal review by the editors, they may be published within a few months of the date of receipt. Style requirements are the same as for regular contributions (see inside back cover).

Spacecraft Structural Model Improvement by Modal Test Results

J.-C. Chen,* L. F. Peretti,† and J. A. Garba‡
Jet Propulsion Laboratory
California Institute of Technology
Pasadena, California

Introduction

Historically, the model modification and updating has been accomplished by a "trial-and-error" approach heavily dependent upon the individual's experience and intuition. With increasing complexity of the structural system, the model modification becomes difficult and systematic approaches are necessary. In recent years, a number of systematic procedures have been developed, typical examples of which are described in Refs. 1-10.

In principle, the procedure uses the differences between the test-measured and analytically obtained eigenvectors and eigenvalues to identify or estimate those model parameters that effect these quantities. The parameters effecting the eigenvalues and eigenvectors are the stiffness and mass representations in the model. In other words, it is the objective of system identification procedure that the stiffness and mass matrices be modified if finite-element formulation is adapted, based on the modal test results. It is common that the measured modal characteristics (namely, the natural frequencies and mode shapes) are used in the identification procedure. However, mode shapes are vector quantities whose elements are the motions of individual degrees of freedom (DOF). For a large, complex structural system, the amplitude of each DOF can be an order of magnitude different. In other words, for certain modes, some dominating DOF will have very large modal displacement and others very little motion. The identification procedure uses the differences between a test-measured mode and a corresponding analytical mode. If the two modes are very close, such that their dominating DOF have the same amplitude and only the less important DOF have different amplitude, the resulting difference between these two vectors will be dominated by those unimportant DOF. This may lead to incorrect parameter identification. The quantities needed to represent the mode shape should be such that the important or dominating DOF are more emphasized than those unimportant DOF.

Received April 12, 1984; presented as Paper 84-1051 at the AIAA Dynamics Specialist Conference, Palm Springs, CA, May 17-18, 1984; revision received March 16, 1986.

*Member of Technical Staff, Applied Technologies Section. Member AIAA.

†Member of Technical Staff, Applied Technologies Section; presently Graduate Student, Duke University.

‡Supervisor, Structures and Dynamics Technology Group, Applied Technology Section. Member AIAA.

In the present study, the kinetic energy distribution is chosen in place of the mode shape for the identification procedure. The kinetic energy is defined as the quantity of modal displacement squared multiplied by the mass associated with the DOF. The idea is to make those DOF with large-mass and/or large-amplitude modal displacement more important than others. The kinetic energy terms specifically eliminate the importance of those large local modal amplitudes associated with very small mass DOF. Also, it is thought that kinetic energy may smooth some of the instrumentation errors by weighting the measurements with the mass matrix. It is believed that this is the first time that kinetic energy is used as measurements in a system identification procedure.

Approach

The approach used in the present study was developed previously.[7] The equation can be written as

$$\{\Delta f\} = \frac{\partial f(r)}{\partial r}\{\Delta r\} \tag{1}$$

where

$$\Delta r_i = r_i - \bar{r}_i$$

$$\Delta f_j = f_j - f_j \tag{2}$$

in which r_i is defined as the ith parameters to be identified (the selected elements in the mass or stiffness matrices in our case), $\bar{r}_i$ the corresponding parameter value used in the analysis (in other words, the values of the elements in the original mass and stiffness matrices); and f_j the jth test measurements such as the eigenvalue or the kinetic energy. It should be noted that the measured quantities such as eigenvalue or kinetic energy are functions of all parameters r_i. Incidentally, the kinetic energy for the jth mode at ith DOF, E_{ij}, is defined as

$$E_{ij} = M_i \phi_{ij}^2 \tag{3}$$

where ϕ_{ij} is the modal displacement at ith DOF of the jth mode. Finally, the matrix $[\partial f/\partial r]$ is referred to as the sensitivity matrix whose elements are the derivatives of the eigenvalues and kinetic energies with respect to the parameters. These derivatives are evaluated at $\bar{r}$.

In Eq. (1), the unknowns are the r_i and the solution involves the inversion of the sensitivity matrix, which usually is not a square matrix. The detailed procedure has been developed in previous studies.[7,11] For the case in which the number of measurements is greater than the number of parameters to be identified, Eq. (1) contains more governing equations than unknowns. The approximate solution is obtained by a minimization procedure and the result is

$$\{\Delta r\} = \left(\left[\frac{\partial f}{\partial r}\right]^T [w] \left[\frac{\partial f}{\partial r}\right]\right)^{-1} \left[\frac{\partial f}{\partial r}\right] [w] \{\Delta f\} \tag{4}$$

where $[w]$ is a positive definite compatible weighting matrix. The purpose of the weighting matrix is to emphasize the important measurements in the identification procedure.

Table 1 Test and analysis modes comparison

Test		TAM6			TAM9			
Mode	Frequency, Hz	Mode	Frequency, Hz	Error,%	Mode	Frequency, Hz	Error,%	Description
1	13.48	1	13.49	0.07	1	13.87	2.89	SXA in x
2	13.69	2	13.74	0.37	2	14.03	2.48	SXA in y
3	17.95	4	18.15	1.11	3	18.48	2.70	Core bending y
4	18.15	5	18.83	3.75	4	18.89	4.08	SXA in x-y
5	18.59	3	16.44	11.57	5	19.56	5.22	Torsion
6	21.60	7	20.52	5.00	7	21.22	1.76	±RTG in z
7	23.58	9	22.97	2.59	8	23.04	2.29	+RTG in z
8	24.85	8	21.27	14.41	10	24.53	1.29	Torsion
14	37.59	17	33.77	10.16	18	37.44	0.40	Bouncing
			Average	5.45		Average	2.57	

Table 2 Orthogonality for test modes

Mode	1	2	3	4	5	6	7	8	14
1	1.00	0.49	0.02	−0.14	0.13	0.07	0.02	−0.03	−0.01
2		1.00	−0.14	−0.10	−0.02	0.06	−0.09	0.00	0.01
3			1.00	0.45	−0.02	−0.04	−0.04	−0.02	0.02
4				1.00	0.16	0.00	0.02	0.02	0.01
5					1.00	−0.02	−0.01	−0.07	−0.04
6						1.00	−0.01	0.02	−0.08
7							1.00	0.02	−0.01
8								1.00	−0.02
14									1.00

Galileo Spacecraft Modal Test

The Galileo is an interplanetary spacecraft whose mission is to conduct scientific exploration of the planet Jupiter. It is to be launched by the Space Shuttle and a modified Centaur upper stage in 1987. The total weight of the spacecraft is approximately 5300 lb. A finite-element model using NASTRAN code was constructed for performing the design loads analysis. This model consists of approximately 10,000 static DOF and 1600 dynamic DOF. It is this loads analysis model that must be verified by the modal test.

Extensive pretest analysis was conducted prior to the modal test[12] for the purpose of understanding the modal characteristics of the loads model. This was essential in such design considerations of the modal test such as the instrumentation distribution and external excitation selection. After careful consideration, it was determined that 162 channels of accelerometer measurements and 118 channels of strain gage measurements would be taken. The instrumentation distribution was such that all of the important modal displacements and modal forces were measured with sufficient resolution. Since the number of DOF in the loads analysis model was a few orders of magnitude greater than the number of measurements to be made during test, a condensed model was constructed such that the DOF would be compatible with the measurements. This condensed model was called the test-analysis model (TAM), which was obtained by the Guyan reduction method to collapse the mass and stiffness matrices in the loads analysis model onto 162 DOF. The TAM was so adjusted that all of the modal characteristics predicted by the loads model should be reproduced by TAM within the range of interest.

The modal test was performed by various testing methods and their detailed descriptions and results can be found in Refs. 13–16. The modal test data chosen for the identification process were obtained from the multishaker sine dwell method because the relative high-amplitude responses are thought to be closer to reality in flight. Of the 17 independent modes obtained by the multishaker sine dwell method, only 9 were used in the identification procedure. They were selected because the large effective masses indicate the global modes. Table 1 lists the frequencies and descriptions of these test modes and those of TAM6. Tables 2 and 3 show the orthogonality and cross-orthogonality, respectively. The analytical mass matrix and modes are those of TAM6.

Subsequent to the modal test, a static test was performed. The results were used to improve the Galileo stiffness matrix. The model improvement and modification were reflected in the TAM7–9. Table 1 also lists the frequencies of TAM9 compared to the test and TAM6. Table 3 also shows the cross-orthogonality between TAM9 and test modes. Figure 1 shows the kinetic energy comparison between the TAM6, TAM9, and the test. According to the test results, TAM9 shows certain improvement over TAM6, but discrepancies still exist.

In view of the corrections of stiffness based on the static test results, the parameters in the identification procedure were limited to the mass representation of the model. Table 4 lists the parameters and their original masses. These parameters are not individual elements in the mass matrices, but rather the lumped masses of several nodes within the major components. All together, 51 test-measured quantities were selected as the observations, which include 9 frequencies and kinetic energies of each of the chosen test modes whose amplitudes exceeded 5%. The sensitivity matrix, whose elements are the derivatives of the eigenvalues and kinetic energies with respect to the parameters, is constructed using perturbation technique outlined in Ref. 7.

The weighting matrix is defined by the effective mass distribution for each mode. The larger effective mass indicates greater paticipation of the mode in the loads analysis; thus, the more important it is. Table 5 shows the effective mass in percentage of the total mass for the nine test modes. The sum of the effective mass over the six directions is the weighting factor for each mode in the weighting matrix $[W]$. Each measurement in the same mode is assigned the same weighting factor and no weighting correlations exist between the modes. Therefore, matrix $[W]$ is diagonal with nine different numbers assigned to nine corresponding modes.

Using Eq. (4), the parameters are estimated and listed in Table 4. Based on the estimated new parameters, a new model was constructed and its eigenproblem solved. It should be noted that one of the parameters (the despun box mass) was identified as having an increment of 290%, which is physically impossible. Therefore, in the new model, a 20% limit was imposed on that parameter. The 20% was chosen because it required only small changes as an a priori condition. Table 6 shows the frequencies calculated from this new model and the comparisons with the test frequencies. In general, the new model is an improvement of the previous model shown in Table 1. The average frequency error is reduced from 5.45 to 1.70%. The orthogonality and cross-orthogonality of the new model are shown in Tables 7 and 8, respectively, to compare the results with those of the previous model shown in Tables 2 and 3. The orthogonality has been improved slightly; however, the major large off-diagonal terms are still present.

Table 3 Cross-orthogonality for test vs TAM6 and TAM9[a]

TAM	Test 1	2	3	4	5	6	7	8	14
1	−0.87	−0.06	−0.15	0.20	−0.16	−0.05	0.02	0.01	0.02
(1)	(0.92)	(0.15)	(0.08)	(−0.18)	(0.20)	(0.03)	(−0.03)	(−0.01)	(−0.02)
2	−0.42	−0.97	0.30	0.22	−0.02	0.01	0.03	0.03	0.02
(2)	(0.34)	(0.97)	(−0.23)	(−0.14)	(0.01)	(−0.01)	(−0.01)	(−0.02)	(−0.02)
4	−0.06	−0.17	−0.88	−0.66	0.02	−0.03	−0.09	−0.03	−0.02
(3)	(−0.07)	(−0.11)	(−0.85)	(−0.77)	(0.05)	(0.00)	(0.01)	(−0.02)	(−0.02)
5	0.16	0.05	0.23	0.48	−0.42	−0.01	0.03	0.03	0.02
(4)	(−0.10)	(−0.01)	(0.44)	(−0.49)	(0.06)	(−0.13)	(−0.04)	(0.01)	(0.00)
3	−0.06	0.02	0.15	−0.45	−0.85	−0.07	0.02	0.02	0.02
(5)	(0.05)	(0.04)	(0.03)	(−0.24)	(−0.91)	(0.12)	(0.09)	(0.09)	(0.02)
7	0.02	0.10	−0.02	0.02	−0.08	0.77	−0.24	−0.02	0.00
(7)	(0.04)	(0.04)	(0.03)	(−0.03)	(0.12)	(0.90)	(0.13)	(−0.07)	(−0.02)
9	−0.01	0.05	0.02	−0.02	−0.02	0.07	−0.60	0.12	−0.01
(8)	(−0.01)	(0.06)	(0.04)	(0.00)	(−0.02)	(0.12)	(−0.75)	(−0.01)	(0.01)
8	−0.02	0.00	−0.02	0.00	−0.02	−0.02	0.09	0.94	0.09
(10)	(−0.01)	(0.02)	(−0.01)	(0.02)	(0.01)	(0.15)	(−0.13)	(0.73)	(0)
17	0.00	−0.02	0.02	−0.01	0.01	0.05	0.01	−0.05	−0.78
(18)	(0.01)	(−0.01)	(0.00)	(0.00)	(0.00)	(0.06)	(0.02)	(0.03)	(−0.70)

[a]Numbers without parentheses are for TAM6; numbers with parentheses for TAM9.

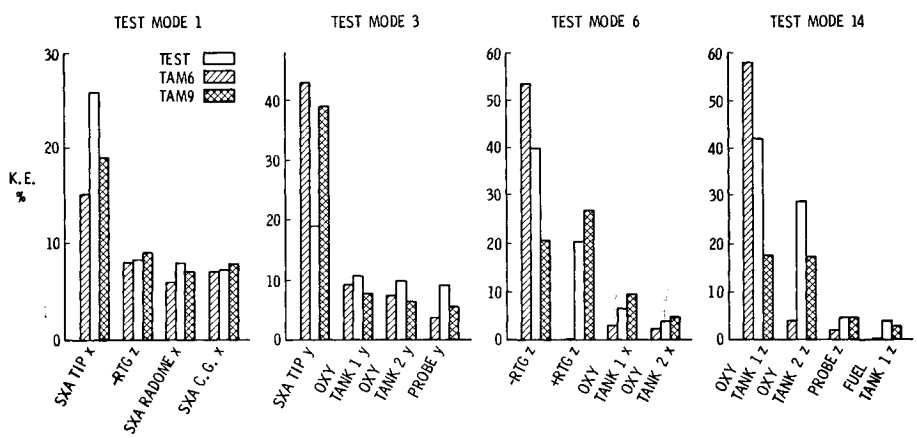

Fig. 1 Kinetic energy distribution for analytical models.

Table 4 Structural parameters

Parameter	Description	Original weight, lb	Identified model: Unweighted — Identified weight, lb	Unweighted — Increment, %	Weighted — Identified weight, lb	Weighted — Increment, %
r_1	SXA	77.92	92.60	18.84	91.36	17.25
r_2	Bus	538.68	452.58	−15.98	342.01	−36.51
r_3	Despun box	217.24	849.34[a]	290.97[a]	753.36[a]	246.79[a]
r_4	Science boom	156.01	155.03	−0.63	163.85	5.03
r_5	Scan platform	207.65	195.72	−5.74	195.92	−5.65
r_6	+X RTG	159.78	161.07	0.81	161.78	1.25
r_7	−X RTG	153.98	156.99	1.95	150.86	−2.03
r_8	Probe	640.41	662.92	3.52	647.81	1.15
r_9	Rpm *Mx, My*	2315.98	2265.80	−2.17	2415.48	4.30
r_{10}	Rpm *Mz*	2315.98	2392.06	3.29	2468.31	6.58

[a]The identified despun box mass is unrealistically high. They are limited arbitrarily to 20% increment in the identified model.

Table 5 Effective mass of test modes

Mode	x	y	z	ρx	θy	θz	Sum[a]
1	0.3695	0.0199	0	0.0356	0.5850	0	1.000
2	0.0231	0.2677	0	0.4011	0.0320	0	0.7239
3	0.0735	0.4456	0	0.3587	0.0550	0	0.9327
4	0.1737	0.2033	0	0.1790	0.1484	0.0548	0.7591
5	0	0	0	0	0.0285	0.2972	0.3257
6	0.2766	0.0103	0.0127	0	0.1346	0.0123	0.4465
7	0	0	0.1018	0.0089	0	0	0.1107
8	0.0133	0	0	0.0022	0	0.3581	0.3737
14	0	0	0.7511	0	0	0	0.7511

[a]Numbers are used in the weighting matrix.

Table 6 Identified modes comparison

Test		Unweighted Model			Weighted Model			
Mode	Frequency, Hz	Mode	Frequency, Hz	Error,%	Mode	Frequency, Hz	Error,%	Description
1	13.48	2	13.54	0.45	2	13.63	1.11	SXA in x
2	13.69	1	13.52	1.31	1	13.56	0.95	SXA in y
3	17.95	4	18.01	0.33	4	18.11	0.89	Core bending y
4	18.15	3	17.85	1.65	3	17.99	0.88	SXA in x-y
5	18.59	5	19.48	4.79	5	19.10	2.74	Torsion
6	21.60	7	21.23	1.71	7	21.26	1.57	±RTG in z
7	23.58	8	22.92	2.80	8	22.93	2.76	+RTG in z
8	24.85	10	24.47	1.53	10	24.54	1.25	Torsion
14	37.59	18	37.33	0.69	18	37.13	1.22	Bouncing
			Average	1.70		Average	1.49	

Table 7 Test modes orthogonality with respect to identified model[a]

Mode	1	2	3	4	5	6	7	8	14
1	1.00	0.49 (0.49)	0.01 (0.01)	−0.06 (−0.06)	0.10 (0.09)	0.06 (0.06)	−0.02 (−0.02)	−0.03 (−0.03)	−0.01 (−0.01)
2		1.00	−0.06 (−0.06)	−0.01 (−0.01)	−0.03 (−0.03)	0.04 (0.04)	−0.07 (−0.07)	0.00 (0.00)	0.01 (0.01)
3			1.00	0.45 (0.44)	−0.02 (−0.03)	−0.05 (−0.05)	−0.04 (−0.04)	−0.02 (−0.02)	0.02 (0.02)
4				1.00	0.16 (0.18)	0.01 (0.01)	0.01 (0.01)	0.02 (0.02)	0.01 (0.01)
5					1.00	−0.03 (−0.02)	−0.01 (−0.01)	−0.06 (−0.05)	−0.04 (−0.03)
6						1.00	−0.01 (0.01)	0.02 (0.02)	−0.09 (−0.10)
7							1.00	0.02 (0.02)	0.00 (0.00)
8								1.00	−0.02 (−0.02)
14									1.00

[a]Numbers without parentheses are for unweighted model; numbers with parentheses for weighted model.

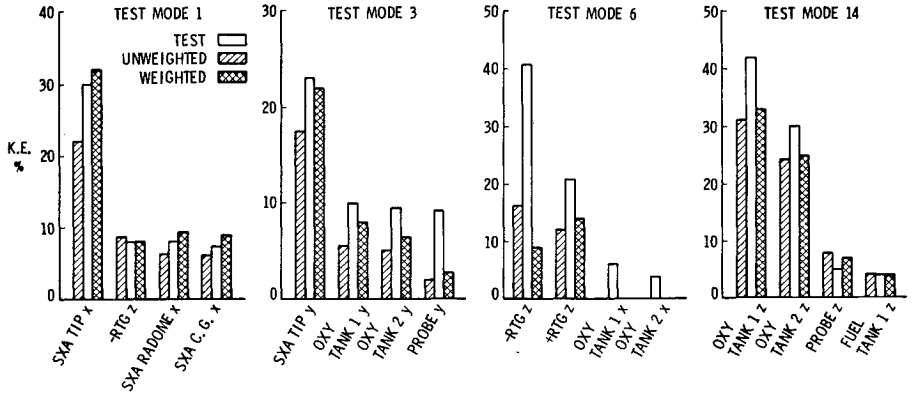

Fig. 2 Kinetic energy distribution for identified models.

Table 8 Cross orthogonality for test vs identified model[a]

Model	Test 1	2	3	4	5	6	7	8	14
2	−0.94	−0.71	0.01	0.04	−0.11	0.00	0.01	0.01	0.02
(2)	(−0.98)	(−0.40)	(0.00)	(0.05)	(−0.11)	(−0.03)	(0.03)	(0.00)	(0.02)
1	0.29	−0.68	0.02	−0.07	0.08	0.05	−0.02	0.01	0.00
(1)	(−0.10)	(−0.90)	(0.02)	(−0.06)	(0.04)	(0.04)	(−0.02)	(0.01)	(0.01)
4	0.00	−0.02	0.83	0.01	0.18	−0.17	−0.06	0.02	0.00
(4)	(0.01)	(−0.01)	(0.74)	(−0.17)	(0.13)	(−0.17)	(−0.07)	(0.02)	(0.00)
3	−0.01	0.01	−0.51	−0.91	0.18	−0.01	0.00	−0.02	−0.02
(3)	(0.00)	(−0.02)	(0.63)	(0.92)	(−0.09)	(0.06)	(0.00)	(0.01)	(0.02)
5	0.03	0.04	0.12	−0.31	−0.89	0.11	0.08	0.07	0.02
(5)	(0.02)	(0.03)	(0.10)	(−0.25)	(−0.92)	(0.07)	(0.08)	(0.06)	(0.02)
7	0.05	0.04	0.05	−0.02	0.14	0.88	0.12	−0.07	−0.02
(7)	(0.05)	(0.05)	(0.04)	(−0.05)	(0.07)	(0.89)	(0.17)	(−0.06)	(−0.02)
8	−0.01	0.07	0.04	0.00	−0.02	0.10	−0.80	−0.01	0.01
(8)	(0.02)	(−0.06)	(−0.04)	(−0.01)	(0.02)	(−0.18)	(0.68)	(−0.02)	(−0.01)
10	0.00	0.03	−0.01	0.02	0.01	0.24	−0.04	0.66	0.00
(10)	(0.01)	(−0.03)	(0.01)	(−0.01)	(0.01)	(−0.19)	(0.15)	(−0.68)	(0.00)
18	−0.01	0.02	0.00	0.01	−0.01	−0.08	−0.02	−0.03	0.91
(18)	(0.00)	(0.02)	(0.00)	(0.01)	(0.00)	(−0.07)	(−0.02)	(−0.03)	(0.92)

[a]Numbers without parentheses are for unweighted model; numbers with parentheses for weighted model.

The improvement on the cross-orthogonality is more evident, especially for the diagonal terms whose values are closer to unity compared with previous models. The kinetic energy comparison is shown in Fig. 2 for the four selected modes. Except for the mode 6, which is a local RTG mode, all of the others show significant improvement.

Conclusions

A system identification procedure has been described and an application to a realistic complex spacecraft structure was performed. The usual modal displacements are replaced by the kinetic energy distributions as the measurement quantities in the procedure. Also, the concept of weighting the measurements in order to emphasize certain data was described. The results show that the proposed approach produces a better model that, in turn, predicts better modal characteristics than the original analytical model.

One shortcoming of the approach is that engineering judgment is still required to eliminate the physically impossible parameter changes. Also, a more important aspect of the approach is the selection of parameters, a process based primarily on the individual's intuition. A more systematic method of selection would be to assign a large number of parameters and to calculate the sensitivity of the modal characteristics with respect to these parameters. Only those with higher sensitivity should be retained for the identification. However, sensitivity calculation is a very expensive process; therefore, it may not be a cost-effective method for a large system containing large numbers of parameters.

Acknowledgment

This research was carried out by the Jet Propulsion Laboratory, California Institute of Technology, under Contract NAS7-918. This task was sponsored by Samuel L. Venneri, NASA Office of Aeronautics and Space Technology.

References

[1]Rodden, W. P., "A Method for Deriving Structural Influence Coefficients from Ground Vibration Tests," *AIAA Journal*, Vol. 5, May 1967, pp. 991-1000.

[2]Berman, A. and Flannelly, W. G., "Theory of Incomplete Models of Dynamic Structures," *AIAA Journal*, Vol. 9, Aug. 1971, pp. 1481-1487.

[3]Pilkey, W. D. and Cohen, R. (eds.), *System Identification of Vibrating Structures, Mathematical Models from Test Data*, American Society of Mechanical Engineers, New York, 1972.

[4]Collins, J. D., Hart, G. C., Hasselman, T. K., and Kennedy, B., "Statistical Identification of Structures," *AIAA Journal*, Vol. 12, Feb. 1974, pp. 185-190.

[5]Garba, J. A. and Wada, B. K., "Application of Perturbation Methods to Improve Analytical Model Correlation with Test Data," SAE Paper 770959, Nov. 1977.

[6]Baruch, M., "Optimization Procedure to Correct Stiffness and Flexibility Matrices Using Vibration Tests," *AIAA Journal*, Vol. 16, Nov. 1978, pp. 1208-1210.

[7]Chen, J. C. and Garba, J. A., "Analytical Model Improvement Using Modal Test Results," *AIAA Journal*, Vol. 18, June 1980, pp. 684-690.

[8]Dobbs, M. W., Balkely, K. D., and Gundy, W. E., "System Identification of Large-Scale Structures," SAE Paper 811050, Oct. 1981.

[9]Berman, A. and Nagy, E. J., "Improvement of Large Dynamic Analytical Model Using Ground Vibration Test Data," AIAA Paper 82-0743, May 1982.

[10]Chen, J. C., Kuo, C. P., and Garba, J. A., "Direct Structural Parameter Identification by Modal Test Results," AIAA Paper 83-0812, May 1983.

[11]Chen, J. C., Peretti, L. F., and Garba, J. A., "Spacecraft Structural System Identification by Modal Test," AIAA Paper 84-1051, May 1984.

[12]Chen, J. C. and Trubert, M., "Galileo Model Test and Pre-Test Analysis," *Proceedings of 2nd International Modal Analysis Conference*, Feb. 1984, pp. 796-802.

[13]Trubert, M., "Assessment of Galileo Modal Test Results for Mathematical Model Verification," AIAA Paper 84-1066, May 1984.

[14]Stroud, R. C., Pamidi, M. R., and Bausch, H. P., "Some Measurement and Analysis Methods Used in the Galileo Spacecraft Modal Survey," AIAA Paper 84-1067, May 1984.

[15]Chen, J. C. and Hunt, D. L., "Application of Multiple Input Random and Polyreference Analysis Techniques to the Galileo Spacecraft Modal Tests," AIAA Paper 84-1069, May 1984.

[16]Pappa, R. S., "Galileo Spacecraft Modal Identification Using an Eigensystem Realization Algorithm Test," AIAA Paper 84-1070, May 1984.